Available online at www.sciencedirect.com

ScienceDirect

Procedia Engineering 213 (2018) 797–803

Procedia Engineering

www.elsevier.com/locate/procedia

7th International Conference on Fatigue Design, Fatigue Design 2017, 29-30 November 2017, Senlis, France

Fatigue lifetime modeling of oxide/oxide composites

Orianne Sally[a,b,c]*, Cédric Julien[b], Frédéric Laurin[b],Rodrigue Desmorat[c], Florent Bouillon[a]

[a] *SAFRAN Ceramics, Rue de Touban, Les cinq chemins, F-33185 Le Haillan, France*
[b] *ONERA -The French Aerospace Lab, 29 avenue de la Division Leclerc, F-92322 Châtillon, France*
[c] *LMT , ENS Paris-Saclay / CNRS / Université Paris-Saclay, 61 avenue du Président Wilson, 94235 Cachan Cedex, France*

Abstract

The assessment of service life of composite thermo-structural parts is a primary issue for the aeronautic industry. To this end, a unified damage model for woven composites undergoing both static and fatigue loadings is presented here. Its specificity resides in its rate damage evolution law, which enables to predict the behaviour of the material under cyclic or random fatigue loadings.

Peer-review under responsibility of the scientific committee of the 7th International Conference on Fatigue Design.

Keywords: Composites; damage model; fatigue lifetime.

1. Introduction

Due to their excellent mechanical properties at high temperatures, ceramic matrix composites (CMC) are often selected for applications in hot part of engines. However, non-oxide composites are severely deteriorated under operating conditions in turbomachines. Consequently, for some engine components subjected to moderate thermo-mechanical loadings (between 800 and 1000°C), oxide/oxide CMCs are potential candidate materials in regard to their interesting trade-off between mechanical properties, thermal stability and cost. Hence, it seems necessary to

* Corresponding author. Tel+33 1 46 73 45 78; fax: +0-000-000-0000 .
*E-mail address:*Orianne.sally@onera.fr

1877-7058
Peer-review under responsibility of the scientific committee of the 7th International Conference on Fatigue Design.
10.1016/j.proeng.2018.02.075

develop efficient computational strategies for the design of composite parts submitted to both static and fatigue loadings.

To fulfil these objectives, a specific damage model for this material has already been developed under static solicitations [1] at Onera but remained to be extended to fatigue loadings. To our knowledge, there is no model in the literature to predict the fatigue lifetime of oxide/oxide materials. A Damage Model for Polymer Matrix Composites, developed at Onera (named ODM-PMC), was recently extended to cyclic fatigue loadings [2] and validated through comparisons with the available experimental data. Nevertheless, some composite parts would be subjected to real fatigue solicitations, not necessarily cyclic, during all the lifetime of an aircraft. Fatigue models using the so-called "kinetic damage evolution law" [3]–[5] allow getting rid of the cycle notion and to handle random complex loadings.

This work presents a unified damage model for woven oxide/oxide composites undergoing static and complex fatigue loadings. The model, described at the woven ply scale (mesoscale), is presented in section 3. The numerical results are then compared to the available experimental data in section 4.

2. Damage model

A model, based on the Continuum Damage Mechanics, was firstly developed to describe the behaviour of oxide/oxide woven ply laminates under static loading.

The model, defined at the woven ply scale, is thermodynamically consistent and is relevant to predict the damage and the failure of oxide/oxide composite structures.

The formulation of the present damage model, is based on previous works performed at Onera and LMT Cachan for composites with polymer matrix or ceramic matrix [1]–[3], [6], [7], but takes into account the specificities of the studied oxide/oxide woven composite material. It is assumed that the observed non-linearities are only due to the damage mechanisms. The macroscopic behaviour, expressed in Eq. 1, derives directly from the Helmholtz free energy.

$$\underline{\sigma} = \underline{\underline{C}}^{eff} : (\underline{\varepsilon} - \underline{\varepsilon}^{th}) - \underline{\underline{C}}^{0} : \underline{\varepsilon}^{r} \quad \text{with} \quad \underline{\underline{C}}^{eff} = \left(\underline{\underline{S}}^{0} + \sum_i d_i \, \underline{\underline{H}}_i \right)^{-1} \tag{1}$$

where $\underline{\sigma}$ is the stress tensor, $\underline{\underline{C}}^{eff}$ the effective elastic stiffness tensor taking into account the effects of the three different damage mechanisms, $\underline{\underline{C}}^{0}$ the initial elastic stiffness tensor, $\underline{\varepsilon}$ the total strain tensor, and $\underline{\varepsilon}^{th}$ the thermal strain tensor. In the present approach, the effects of damage mechanisms (in-plane transverse cracking in the matrix in the warp or weft direction and yarn/matrix deboundings) on the macroscopic behaviour are translated by an increase of the initial elastic compliance $\underline{\underline{S}}^{0}$ with an additional term ($\sum d_i \underline{\underline{H}}_i$), that depends on the damage variables and the corresponding effect tensors, describing the effects of an open crack on the effective stiffness. Finally, the specific strain tensor $\underline{\varepsilon}^{r}$ accounts for the residual strains after unloading, due to the evolution of the different damages.

2.1. Damages occurring during static loadings

Ben Ramdane [1] demonstrated experimentally that the damage in this material is mainly oriented by the microstructure. Therefore, under plane stress hypothesis (representative conditions of the available tests), only two scalar damage variables, d_1 and d_2, are introduced in the model, corresponding respectively to the in-plane damages within the matrix oriented in the warp and in the weft directions.

The driving forces y_k associated to the damage variables (see Eq. 2) have been formulated in a so-called non-standard thermodynamic framework.

$$\begin{cases} y_1 = \frac{1}{2}\left(C_{11}^0 \varepsilon_1^{+^2} + a_{26}\varepsilon_6^{+^2} \right) \\ y_2 = \frac{1}{2}\left(C_{11}^0 \varepsilon_2^{+^2} + a_{16}\varepsilon_6^{+^2} \right) \end{cases} \quad \text{and} \quad X_{y_k} = \sqrt{y_k} \tag{2}$$

They depend on (i) the different components of the initial elastic stiffness tensor, (ii) the parameters a_{16} (resp. a_{26}) which couples damage induced in the warp (resp. weft) direction to in-plane shear and (iii) on the specific positive strain tensor. The positive strain tensor, associated to the driving forces, corresponds to the positive part, as proposed by [2], of the total strain tensor, where all the components are zeros except those inducing damage.

The damage evolution laws of the two variables, expressed in Eq. 3, are formulated as kinetic damage laws and derive directly from those described in [1], [2].

$$\dot{d}_k^{\,static} = (d_{ck} - d_k)\left(\frac{< X_{y_k} - X_{y_{0k}}^s >}{S^s{}_k} \right)^{p_k^s} \dot{X}_{y_k} \quad \text{and} \quad k = \{1,2\} \tag{3}$$

where d_{ck} corresponds to the saturation of the damage, ($S^s{}_k$, $p^s{}_k$) are parameters, which allow to calibrate the damage evolution laws. $X_{y_{0k}}^s$ is related to the damage threshold that is taken into account by the mean of the positive parts <.> (classical Macauley brackets). X_{y_k} is linked to the equivalent driving forces y_k (Eq. 2) and evolves linearly as a function of the applied strain. It can be noted that the damage is only allowed growing, in order to ensure the second principle of thermodynamics.

Let us note that no yarn fibre failure criterion has been taken into account here; but it will be included in future work. Only the evolution of the macroscopic behaviour due to damages is considered in the present paper.

2.2. Damages occurring during fatigue loadings

Previous works on PMCs [8] showed that damage induced by static or fatigue loadings have the same morphologies, effects on the behaviour and damage saturation level, but have different evolution (damage induced by fatigue loadings evolves much more slowly than those induced by static loadings). Thus, to extend the model to fatigue loadings, only the damage evolution laws are modified. As a consequence, the framework used in the previous paragraph is still valid for the damage evolution law.

Due to the similarity between the evolution laws of the two types of loadings, it is possible to merge the contributions from both the static and fatigue solicitations into a single damage evolution law. By extension, a single damage variable for each degradation mechanism can be used. The rates of the contributions of static and fatigue damage are cumulated as follows (Eq. 4):

$$\dot{d}_k = (d_{ck} - d_k)\left(\frac{< X_{y_k} - X^s_{y_{0k}} >}{S^s_k}\right)^{p^s_k} \dot{X}^{\max}_{y_k} + (d_{ck} - d_k)^{\gamma_k}\left(\frac{< X_{y_k} - X^f_{y_{0k}} >}{S^f_k}\right)^{p^f_k} (< \dot{X}_{y_k} >_+ - \dot{X}^{\max}_{y_k}) \quad (4)$$

where d_{ck} and (S^s_k, p^s_k) are identical to those expressed in Eq. 3. Furthermore, (γ_k, S^f_k, p^f_k) are parameters, which permit to calibrate damage evolution laws during fatigue loading. Additionally, γ_k can be obtained easily from a fatigue curve in the direction *k*. $X^f_{y_{0k}}$ is related to the fatigue threshold, which is lower or equal to the static threshold. The damage law (Eq. 4) is based on the previous work of Angrand developed for PMC materials [3].

The evolution of $\dot{X}^{\max}_{y_k}$, which is the evolution of maximum value of X_{y_k} over the entire loading, permits to switch between the static and fatigue evolution, as illustrated in Fig. 1. When the maximum load increases, the static contribution is activated. Conversely the fatigue contribution is activated while the load maximum is not exceeded, but the driving force increases and is higher than the fatigue threshold. For instance, the first load increase in Fig. 1(b) is a static charge ($X^{\max}_{y_k}$ increases and the first part of Eq. 4 is activated) and static damage evolves from the static threshold to the peak. During discharge, no damage is created. Then, as the load increases again, fatigue damage occurs once the fatigue threshold is reached ($X^{\max}_{y_k}$ keeps the same value whereas X_{y_k} increases: the second part of Eq. 4 is activated). In case of X_{y_k} becomes higher than the previous value of $X^{\max}_{y_k}$ ($\dot{X}^{\max}_{y_k}$ thus evolving), the damage evolution is due to the static contribution of Eq. 4.

This kinetic formulation enables naturally the model to simulate any kind of loading, static, cyclic (Fig. 1(a)) or complex ones (Fig. 1(b)).

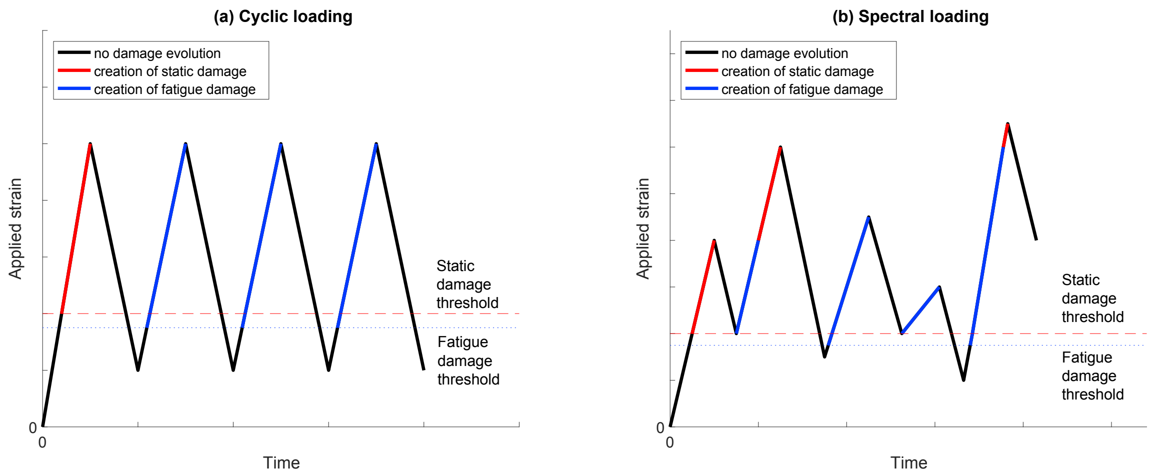

Figure 1 : Evolution of the different damage contributions activated during cyclic or complex fatigue loading

3. Comparison with test results

All the tests were performed by SAFRAN Ceramics on laminates constituted with eight oxide/oxide woven plies oriented at 0°. The woven fabric was an eight-harness satin weave. The fabric is assumed to be balanced and, in that regard, the warp and weft parameters are considered identical.

3.1. Static tests

The static parameters, appearing in Eq. 3, were identified thanks to three experimental stress/strain curves:

- a monotonic tensile test at 0°, where the non-linearities are only due to d_1
- a monotonic tensile test at 45°, where the non-linearities are due to both d_1 and d_2
- an incremental tensile test at 45°, which shows the necessity to insert residual strain in the model.

Fig. 2 compares model predictions and experimental data in the three cases.

Good agreement was found between the experimental data and the results of the simulations in term of non-linear behaviour, which confirmed the ability of the model to describe the macroscopic behaviour of laminated oxide/oxide materials. A fine description of the non-linear behaviour is necessary to be able to perform finite element structure computations, which is the aim of this study.

Let us note nonetheless that in Fig. 2(c) the initial slope of the incremental tensile test differs from that of the monotonic test due to material dispersion. Moreover, the material variability was not taken into account, since only one test for each configuration was available.

To simulate the static behaviour of a representative volume element, the computational time is about few seconds.

3.2. Fatigue tests

As for determining the fatigue behaviour of the material, fatigue tests have been performed under imposed stresses conditions in the warp direction. The stress ratio R ($R = \frac{\sigma^{\min}}{\sigma^{\max}}$) was set at 0.05 and the frequency to 10 Hz.

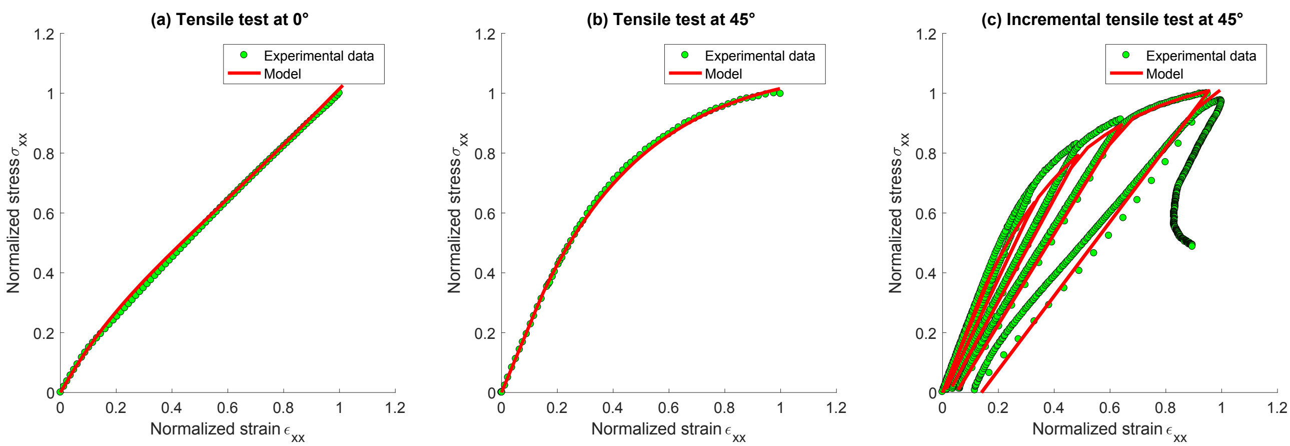

Figure 2: Comparison between model and experimental data for static tests.

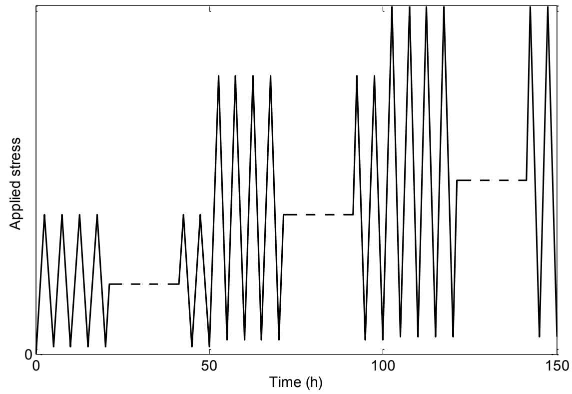

Figure 3: Evolution of the applied fatigue loading

The test consists of several floors of increasing applied maximal stress with a constant ratio after a given number of cycles (around 1.8 million of cycles), as shows Fig. 3.

It is then necessary to identify an appropriate set of fatigue parameters as well as static parameters in order to compute the evolution of the secant modulus. The experimental and simulated results were compared after identifying the parameters specific to fatigue damage in Eq. 5, on a 0° ply subjected to fatigue loadings.

The results of the simulations are shown in Fig. 4: the panel (a) shows the comparison between test results and numerical calculations throughout the three first stages while the panel (b) focuses on the first load stage. Currently, all the cycles during fatigue phases are simulated but also the static part between each fatigue phases.

The general trend of the secant modulus (defined as $E^{sec} = \frac{\sigma^{max}}{\varepsilon^{max}}$ for each cycle) versus time is well captured, particularly during the first two load stages. We can also note that the loss of modulus due to the change of maximum stress (during static loading) seems to be accurate.

The results are satisfactory given the current state of development of the model. The mean stress effect [4] is not yet taken into account, which leads to neglecting the load history and explains probably why the third stages is not accurately described. This point will be considered in future works.

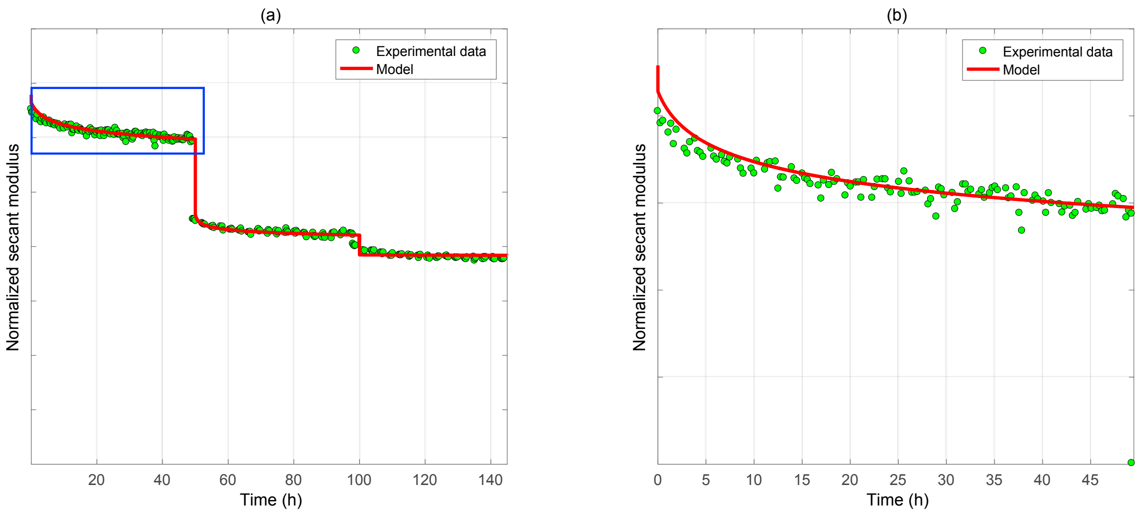

Figure 4: Comparison of the model predictions and the experimental data on (a) the whole fatigue test and (b) only the first stage

4. CONCLUSION/PERSPECTIVES

To design oxide/oxide composites parts, it is necessary for the industrials to use physically based damage models, available in a finite element code.

In that perspective, the proposed damage model allows to describe the evolution of damage under static and/or fatigue loadings and a first identification of its parameters have been performed. The fatigue loading can be cyclic or spectral thanks to the kinetic formulation of the damage evolution law, which can naturally handle complex loadings.

The calculation costs of fatigue tests remain too high for an industrial use in the case of fatigue polycyclic tests. This is the reason why the damage evolution law should be associated to efficient computational strategies, such as cycles jumps [9], in order to reduce the computational time and to allow considering composite components. Then, this model will be implemented in a commercial finite element code for large structural applications subjected to complex fatigue loading.

Acknowledgements

The collaboration with SAFRAN Ceramics is gratefully acknowledged. This work was supported under PRC MECACOMP, French research project co-funded by DGAC and SAFRAN Group, piloted by SAFRAN Group and involving SAFRAN Group, ONERA and CNRS.

References

[1] C. Ben Ramdane, “Etude et modélisation du comportement mécanique de CMC oxyde/oxyde,” Bordeaux, 2014.

[2] C. Rakotoarisoa, “Prévision de la durée de vie en fatigue des composites à matrice organique tissés interlock,” Université de Technologie de Compiègne, 2014.

[3] L. Angrand, “Modèle d’endommagement incrémental en temps pour la prévision de la durée de vie des composites tissés 3D en fatigue cyclique et en fatigue aléatoire,” Université Paris-Saclay, 2016.

[4] R. Desmorat, L. Angrand, P. Gaborit, M. Kaminski, and C. Rakotoarisoa, “On the introduction of a mean stress in kinetic damage evolution laws for fatigue,” *Int. J. Fatigue*, vol. 77, pp. 141–153, Aug. 2015.

[5] J. Lemaitre, J. P. Sermage, and R. Desmorat, “A two scale damage concept applied to fatigue,” *Int. J. Fract.*, vol. 97, no. 1, pp. 67–81, 1999.

[6] E. Hemon, “Modèles multi-niveaux de prévision des durées de vie en fatigue des structures composites à matrice céramique pour usage en turbomachines aéronautiques,” Université Sciences et Technologies-Bordeaux I, 2013.

[7] L. Marcin, “Modélisation du comportement, de l’endommagement et de la rupture de matériaux composites à renforts tissés pour le dimensionnement robuste de structures,” Université Bordeaux 1, 2010.

[8] N. Revest, “Comportement en fatigue de pièces épaisses en matériaux composites,” École Nationale Supérieure des Mines de Paris, 2011.

[9] W. Van Paepegem, J. Degrieck, and P. De Baets, “Finite element approach for modelling fatigue damage in fibre-reinforced composite materials,” *Compos. Part B Eng.*, vol. 32, no. 7, pp. 575–588, Oct. 2001.